J. Plasma Phys. (2024), *vol*. 90, 975900206
Published by Cambridge University Press
doi:10.1017/S0022377824000515

Recent results on high-β plasma confinement studies in the Gas Dynamic Trap

Evgeniy A. Shmigelsky [1,2,†], Andrej A. Lizunov [1,2], Andrey K. Meyster [1], Egor I. Pinzhenin [1], Alexander L. Solomakhin [1,2] and Dmitry V. Yakovlev [1,3]

[1]Budker Institute of Nuclear Physics, Lavrentyev avenue 11, Novosibirsk 630090, Russia

[2]Novosibirsk State University, Pirogov street 1, Novosibirsk 630090, Russia

[3]University of Wisconsin-Madison, Madison, WI 53706, USA

(Received 29 December 2023; revised 2 April 2024; accepted 2 April 2024)

This paper is devoted to experimental studies of plasma confinement with high relative pressure (β) in the Gas Dynamic Trap (BINP, Novosibirsk). In previous high-β confinement studies a maximum local $\beta = 0.6$ was achieved in the fast-ion turning point, contributed to by a beam-driven population of fast ions with an anisotropic distribution function. In this study the axial magnetic field profile was modified to bring the turning points closer to one another, which effectively increased the energy density of plasma and pushed the β value higher. Experiments were performed for two non-standard magnetic configurations, where the axial fast-ion confinement region length was reduced by 1.5 and 2 times compared with the standard configuration. The average values of $\langle\beta_\perp\rangle$ over the plasma central cross-section were found to be 0.1 and 0.18, respectively, for the two configurations, with the latter value significantly exceeding the $\langle\beta_\perp\rangle = 0.08$ of the standard configuration, in which the previous record was set. Moreover, halving the fast ion confinement region almost doubled the D–D fusion proton flux from the trap centre compared with the standard configuration. The electron temperature in both new magnetic configurations was only slightly smaller than in the standard configuration. In addition, an effect of Alfvén ion–cyclotron instability (AICI) development on the pressure in the turning points is discussed. Presumably, with some decrease in magnetic field an evolving AICI does not result in considerable pressure axial redistribution, so the pressure maximum is in the turning points' vicinity despite the instability.

Keywords: plasma confinement, plasma instabilities

1. Introduction

The Gas Dynamic Trap (GDT) in the Budker Institute of Nuclear Physics, Novosibirsk (Ivanov & Prikhodko 2017) is an axisymmetric open magnetic trap involved in studies aimed at improving the plasma confinement in open magnetic traps for such prospective technological applications as a volumetric fusion neutron source or a thermonuclear power plant (Bagryansky *et al.* 2020; Skovorodin *et al.* 2023).

† Email address for correspondence: e.shmigelskii@g.nsu.ru

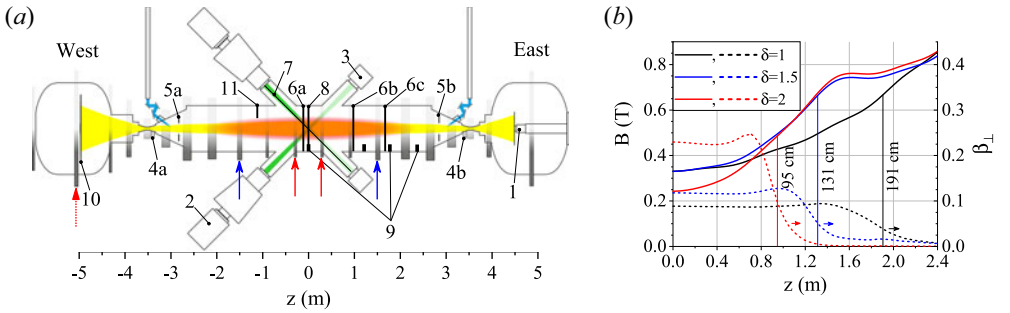

FIGURE 1. (*a*) Layout of the GDT with its main parts and diagnostics: 1, arc plasma generator; 2, NBI; 3, secondary electron emission detector set; 4a, 4b, gas valves; 5a, 5b, annular limiters; 6a, 6b, 6c, diamagnetic loops; 7, dispersion interferometer's line of sight; 8, Thomson scattering system's line of sight; 9, proton detectors; 10, diagnostic plasma absorber; 11, azimuthal magnetic probe array. Blue and red arrows point out the coils involved in magnetic field profile modifications. (*b*) Axial profiles of magnetic field (left-hand axis) and $\beta_\perp$ calculated with the DOL code (right-hand axis) for the cases of various magnetic configurations denoted by parameter δ.

The competitive advantage of open traps is the principal possibility of them confining plasma under relative pressure $\beta = 8\pi p/B^2$ approaching unity. At $\beta \to 1$, open systems for plasma confinement utilise the external magnetic field most effectively, thus having the potential for designing compact fusion devices. More importantly, the thermonuclear yield for the gas-dynamic confinement is proportional to $\beta/\sqrt{1-\beta}$ since the effective mirror ratio increases as $\beta \to 1$. As shown in Beklemishev (2016) and Khristo & Beklemishev (2022), there is a so-called 'diamagnetic bubble' equilibrium configuration when $\beta \to 1$, in which the energy confinement time has to significantly exceed the gas-dynamic time.

Plasma pressure in the GDT is concentrated in the fast-ion population that originates from charge exchange between the initial plasma target and injected neutral beams, and has an anisotropic distribution function. These particles, also called 'sloshing' ions, are confined adiabatically and have their pressure maxima located at the turning points in the absence of micro-instabilities. Confinement of fast ions under local β approaching 0.6 in the turning points has been demonstrated in Bagryansky *et al.* (2011). Further increase of the confined ion pressure to achieve larger β and face unexplored phenomena in this parameter space is the actual problem. One way to increase β without upgrading the injection system is to enhance the energy density of the fast ions, which can be done by decreasing their movement region.

In this paper we set goals to study the plasma confinement in the GDT in several new magnetic configurations with shortened regions of fast-ion movement in general and to achieve the maximum plasma pressure. It is equivalent to the maximisation of the magnetic flux excluded by the plasma, i.e. diamagnetic flux.

2. Experimental set-up

The main heating system of the GDT is a set of eight neutral beam injectors (NBIs) with mean energy 24 keV and the total of power up to 5 MW (2 in figure 1*a*). The beams are inclined at 45° to the trap axis, so the fast ions' turning points correspond to coordinates where the magnetic field strength is twice as high as in the central plane, that is, the points where the local mirror ratio R equals 2. The neutral beams' impact parameter in relation to the GDT axis is set equal to the gyroradius of newly injected fast ions with 24 keV energy

https://doi.org/10.1017/S0022377824000515 Published online by Cambridge University Press

for the central magnetic field of 0.35 T. The magnetic field strength in our experiments was varied from 0.24 to 0.33 T, so the gyroradius of 24 keV ions exceeds the impact parameter by 46 % or 6 % for those field strengths, respectively.

To implement confinement regimes with narrower magnetic wells in comparison with the standard axial profile of the magnetic field, two reversible modifications of the GDT magnetic system were made. Each magnetic configuration is denoted hereinafter by the parameter δ, which denotes the relation between the distance between the turning points, calculated for vacuum magnetic fields in the standard configuration, and the same for the configuration which is being referred to. The first modification is the commutation of specially constructed 'double' coils (indicated by blue arrows in figure 1*a*) in the mode with doubled number of turns. This action brings turning points closer than in the standard configuration ($\delta = 1$), so the parameter $\delta = 1.5$ in such a case. The second step is to connect the central pair of coils (red arrows in figure 1*a*) in parallel, changing the configuration with $\delta = 1.5$ into one with $\delta = 2$.

Figure 1(*b*) shows axial profiles of magnetic field for all three mentioned configurations. These profiles were used to calculate axial profiles of $\beta_\perp$ (figure 1*b*, dashed lines, right-hand axis) with the DOL code (Yurov, Prikhodko & Tsidulko 2016). The computations were tuned to provide coincidence of experimental and calculated time dependencies for diamagnetic flux in the central plasma cross-section and captured NBI power as well as approximate correspondence between electron temperatures. According to computed locations of the axial pressure profiles' maxima, degrees of shrinking of the fast-ion movement region are 1.4 and 1.9 for configurations $\delta = 1.5$ and $\delta = 2$, respectively. The DOL code is one-dimensional in coordinate space, so calculated $\beta_\perp(z)$ can be considered as the relative pressure averaged over the plasma cross-sections. Consequently, one can see that in the central section the average $\beta_\perp$ in configuration with $\delta = 1.5$ is 1.3 times more than in the standard configuration. Moreover, calculated $\beta_\perp$ is 2.6 times higher for the case of $\delta = 2$.

The following sequence occurs during each discharge (figure 2). Deuterium is puffed mainly from the eastern gas valve (4a in figure 1*a*) and sometimes from the western one (4b) to further increase the plasma density. Plasma density is set by varying the start times and puffing duration as well as the pressure of the gas puffing. Then the arc plasma generator (1 in figure 1*a*) creates cold deuterium plasma that serves as the target for capture of deuterium neutral beams' power. Applying voltage to limiters (5a, 5b in figure 1*a*) is necessary to avoid magnetohydrodynamic disruptions of the plasma (Beklemishev *et al.* 2010).

Alfvén ion–cyclotron instability (AICI) (Zaytsev *et al.* 2013, 2014; Anikeev *et al.* 2015) develops during each discharge (see figure 2*c*) under the confinement conditions in which we are interested and provokes scattering of fast ions and relaxation of their distribution function. This manifests in rapid restructuring of the fast-ion axial pressure profile which looks like a sharp change in diamagnetic fluxes, especially near the turning points (see figure 2*b* at 6.25 ms). Such a restructure is accompanied by 'impact' excitation of the global acoustic mode (figure 2*d*) (Skovorodin, Zaytsev & Beklemishev 2013) at a frequency equal to ≈150 kHz whose value is approximately 1.5 times higher than that reported in the paper cited that is in agreement with the shrinking of the fast-ion movement region in the configuration with $\delta = 1.5$.

Several parameters were used to monitor confinement conditions in general. The main parameter is the maximum value of the diamagnetic flux $D_{\max}$ since this flux is proportional to average transverse pressure $D \sim \langle p_\perp / B \rangle$. The diamagnetic flux is measured by a diamagnetic loop (6a in figure 1*a*) located 14 cm away from the central plasma cross-section. Henceforth we equate the loop's plane with the central plane since the axial

https://doi.org/10.1017/S0022377824000515 Published online by Cambridge University Press

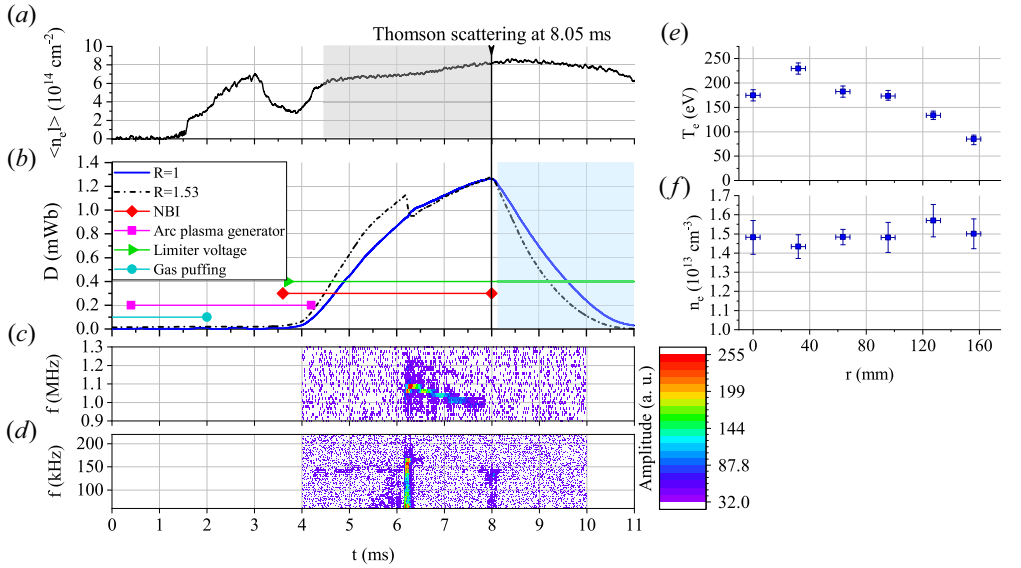

FIGURE 2. Characteristic sequence of processes during plasma discharge in the example shot no. 52889 in configuration $\delta = 1.5$. Time dependencies of (*a*) linear density $\langle n_e l \rangle$ and (*b*) diamagnetic fluxes D measured in different planes along the trap axis defined by local mirror ratio values R. (*c*) Magnetic probe and (*d*) diamagnetic loop signal spectrograms demonstrate the presence of the AICI and the global sound mode, respectively. Radial profiles of the (*e*) electron temperature and (*f*) density at the end of NBI in the central GDT plane.

profiles of various plasma parameters have to be uniform near the symmetry plane and the distance to the turning point from the centre is much greater than the distance between these two planes. Although fast-ion pressure has to be the highest at the turning point's vicinity, the central plane is more appropriate because of the possibility of comparing magnetic configurations despite different locations of the turning points and since plasma pressure in the central plane is less affected by pressure profile restructuring due to AICI than near the turning points. Besides, since we measured diamagnetic flux at two other planes along the axis (6b, 6c in figure 1*a*), we can make qualitative conclusions about time evolution of the fast-ion pressure axial profile.

The rate of diamagnetic flux decay indicates the fast ions' energy losses rate. This is formalised by the parameter $\tau_{\text{decay}} = \langle (t - t_1)/\ln[D(t_1)/D(t)] \rangle$, where $\langle \cdots \rangle$ means averaging over an interval of $t_1 \leq t \leq t_2$ of the diamagnetic flux's decay stage (shaded area in figure 2*b*) and $D(t)$ is the diamagnetic flux in the central plane. Since decrease of the flux is not exactly exponential, τ_{decay} values have error bars that show the standard deviation.

Next, each discharge is characterised by the linear electron density of the plasma $\langle n_e l \rangle$ averaged over section from 4.5 to 8 ms (shaded area in figure 2*a*) and trapped NBI power $\langle P_{\text{tr}} \rangle$ averaged over the injection time. The dispersion interferometer and secondary electron emission detectors were used to measure these values (7 and 3 in figure 1*a*, respectively). Discharge operation was set up so that linear density grew during the injection; thus the standard deviation is large enough and shows the degree of the growth. Error bars of $\langle P_{\text{tr}} \rangle$ are omitted.

In addition, each confinement regime is described by measurements of electron temperature T_e and density n_e along the radius using a Thomson scattering system

https://doi.org/10.1017/S0022377824000515 Published online by Cambridge University Press

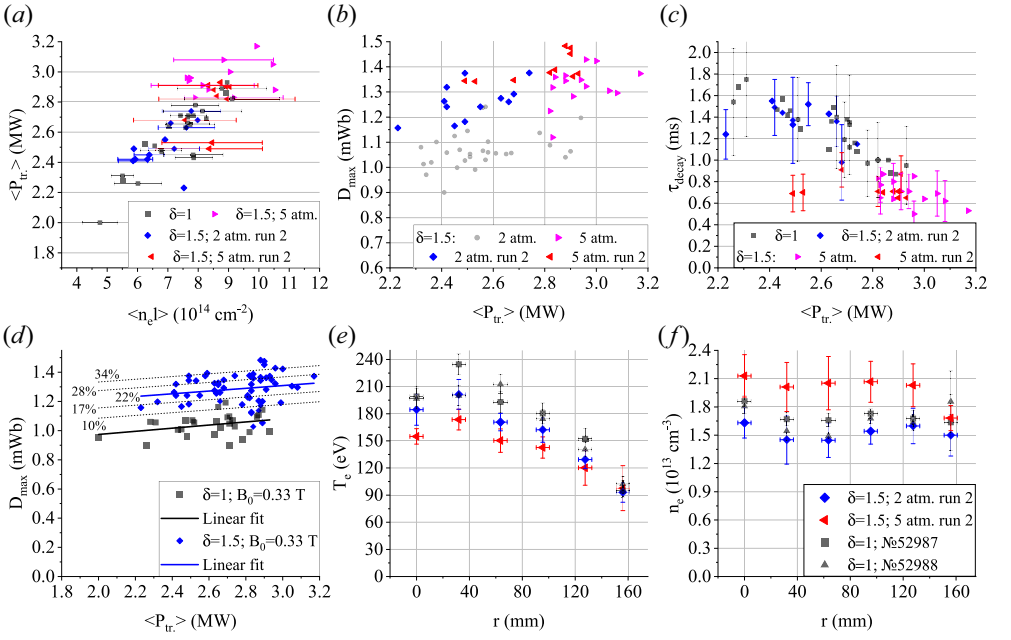

FIGURE 3. Comparison of two confinement regimes (moderate and enhanced gas puffing) in the $\delta = 1.5$ configuration: (*a*) dependence of trapped NBI power on linear density, both averaged over NBI duration, and dependencies of (*b*) the maximum diamagnetism (in the central plane) and (*c*) its decay time after NBI on trapped NBI power. Comparison of confinement in magnetic configurations with $\delta = 1$ and $\delta = 1.5$: (*d*) dependence of maximum diamagnetism on trapped NBI power; radial (*e*) electron temperature and (*f*) density profiles.

(Lizunov *et al.* 2023) in the central plane (8 in figure 1*a*). Figures 2(*e*) and 2(*f*) demonstrate typical T_e and n_e radial profiles in the configuration with $\delta = 1.5$. The temperature has a maximum of 230 eV at a radius of 32 ± 5 mm and equals 85 eV at a radius of 156 ± 5 mm which corresponds to the limiter projection to the central plane. Density n_e has a uniform radial distribution right up to the limiter projection. This and the off-axis maximum of $T_e(r)$ are common features of all T_e and n_e radial profiles that are considered in this paper.

Error bars of n_e and T_e below refer to measurement errors for the case of specific discharges (as in figures 2*e*, 2*f*, 3*e* and 3*f*). Whereas n_e and T_e profiles without any discharge number are averaged over from 4 to 14 profiles measured near the moment when diamagnetic flux has a maximum and under the same discharge conditions. Their error bars are the standard deviations.

3. Results

3.1. *Comparison of plasma confinement under $\delta = 1.5$ and $\delta = 1$*

A series of discharges was devoted to formation of target plasma of such density as to capture as much NBI power as possible. To do this, we raised the pressure in the gas reservoir, connected to the valve by 3 atm and then by 5 atm instead of usual 1 or 2 atm. The start and duration times of gas puffing were set up to provide the highest possible fraction of trapped power during NBI, and it turned out to be growing with time, especially for puffing at 5 atm. In figure 3(*a*) the dependence of $\langle P_{\rm tr}\rangle$ on $\langle n_e l\rangle$ averaged over the interval from 4.5 to 8 ms is shown. Puffing at 5 atm allowed us to capture up to 3.2 MW of

https://doi.org/10.1017/S0022377824000515 Published online by Cambridge University Press

NBI power, which is 75 % of the total power. Here (figure 3) and below the designation 'run 2' means discharges in the configuration with $\delta = 1.5$ that were conducted when the inner ring of the western plasma absorber was grounded. Discharges in other configurations were also conducted with the inner ring grounded.

An enhancement of the trapped NBI power with massive gas inflow at 5 atm leads to higher $D_{\max}$ compared with moderate gas puffing at 2 atm as can be seen in figure 3(*b*). In addition, figure 3(*f*) demonstrates ≈40 % higher electron density for massive inflow compared with the moderate inflow. However, the decay time of diamagnetic flux τ_{decay} significantly decreases (figure 3*c*) and T_e (red points in figure 3*e*) turns out to be smaller with a large amount of gas. These observations provide evidence of additional transverse losses of fast ions due to charge exchange with excess neutral gas. The available method to increase the trapped power necessarily causes a higher rate of energy losses. Therefore, moderate gas puffing at 2 or 3 atm looks more reasonable, especially because $D_{\max}$ does not decrease much.

Let us consider plasma confinement in configurations with $\delta = 1.5$ and $\delta = 1$ in relation to one another. The supply voltage of the GDT central solenoid was decreased in the standard configuration to make the central on-axis magnetic field the same as in the $\delta = 1.5$ configuration. Therefore, in both configurations the central magnetic field was equal to 0.33 T. Decay times τ_{decay} (figure 3*c*) coincide for operation under $\delta = 1$ and $\delta = 1.5$, when plasma densities n_e are regular and almost the same, though T_e is slightly smaller for the case of $\delta = 1.5$ (see black and blue symbols in figure 3*e*,*f*).

Figure 3(*d*) contains maximum values of diamagnetic flux $D_{\max}$ in the central plane for both configurations despite different operational conditions. These points were fitted by straight lines, and their slopes turned out to be almost the same; therefore, the absolute difference between both fitted lines does not depend on $\langle P_{\text{tr}} \rangle$ and relative difference equals 22 % at $\langle P_{\text{tr}} \rangle = 2.6$ MW. Since $D_{\max}$ values are highly spread, additional dotted lines are added to figure 3(*d*) in order to show variability of relative difference. As a result, transversal pressure of fast ions on average across the central section is 22 % higher when the turning points are 1.5 times closer to each other ($\delta = 1.5$), although the T_e profile lies below that of the standard configuration.

3.2. *Confinement under* $\delta = 1.5$ *and low* B

Experiments in configuration $\delta = 1.5$ were continued by a study of plasma parameters with a lower-than-usual magnetic field. Such a study is motivated by the need to determine whether AICI manifests differently in lower B than under default B. Indeed, it is shown in Zaytsev *et al.* (2013) and Tsidulko & Chernoshtanov (2014) that the β threshold of AICI increases when magnetic field decreases. Moreover, as had been discovered in earlier experiments on the GDT (Bagryansky *et al.* 2011), the maximum local $\beta = 0.6$ (measured with spatial resolution of 3 cm) in the turning point took place when B was equal to 0.28 T in the central plane (Simonen 2016).

To be able to compare regimes with various magnetic fields, values of $D_{\max}$ are recalculated into $\langle \beta_\perp \rangle$ as follows. Using the paraxial equilibrium approximation applicable for the GDT case, we can write an expression $B_{\text{pl}} = B\sqrt{1 - \beta_\perp}$ that links B (magnetic field in the absence of plasma), B_{pl} (magnetic field weakened by the plasma diamagnetism) and $\beta_\perp$. Then we assume that most of the fast ions are distributed inside the magnetic surface enclosed radially by the limiters (4a and 4b in figure 1*a*). In this case $D = (B - \langle B_{\text{pl}} \rangle) S_{\text{pl}}$, where $\langle \cdots \rangle$ means averaging over the plasma cross-section in the central plane which has an area of the limiting magnetic surface equal to S_{pl}, and $\langle B \rangle = B$ because of uniformity of vacuum magnetic field. Here $\langle B_{\text{pl}} \rangle$ can be used to give meaning to $\langle \beta_\perp \rangle$ in this way:

https://doi.org/10.1017/S0022377824000515 Published online by Cambridge University Press

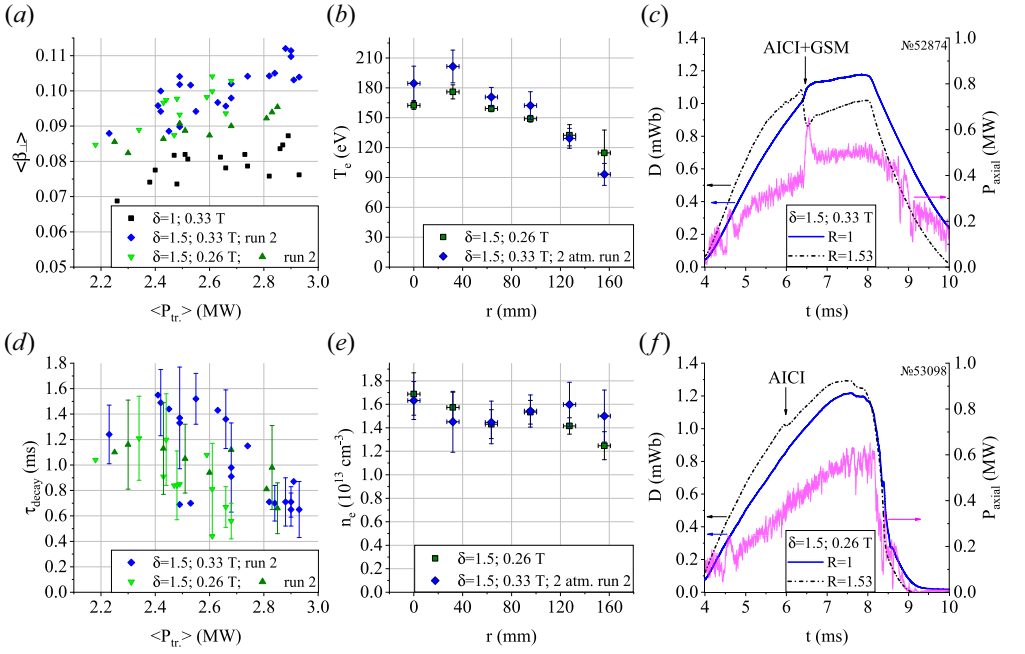

FIGURE 4. Confinement regimes with standard ($B = 0.33$ T) and low ($B = 0.26$ T) magnetic field strengths in the $\delta = 1.5$ configuration. Average (*a*) β and (*d*) τ_{decay} versus trapped NBI power. Radial (*b*) T_e and (*e*) n_e profiles. Time dependencies of diamagnetic flux at two planes denoted by the value of local mirror ratio R and axial power losses in the case of (*c*) standard B and (*f*) low B.

$\langle B_{\text{pl}}\rangle = B\sqrt{1-\langle\beta_\perp\rangle}$. Indeed, with this definition $\langle\beta_\perp\rangle$ is not a real $\beta_\perp$ distribution average, but it is related to the average magnetic field generated by plasma. From the above expressions one can derive the following:

$$\langle\beta_\perp\rangle = \frac{D_{\max}}{BS_{\text{pl}}}\left(2 - \frac{D_{\max}}{BS_{\text{pl}}}\right). \tag{3.1}$$

The regime with lowered magnetic field $B = 0.26$ T was studied the most thoroughly. Figure 4 shows values of $\langle\beta_\perp\rangle$ for this case as well as for default magnetic field. It is seen that values $\langle\beta_\perp\rangle$ are not higher for $B = 0.26$ T than for $B = 0.33$ T. Wheras, τ_{decay} in figure 4(*d*) is systematically smaller in the case of low B up to $\langle P_{\text{tr}}\rangle = 2.8$ MW, where transverse losses are not yet very high. Besides, when n_e for regimes with these two magnetic fields are comparable, T_e turns out to be smaller near the axis, but the same and even higher in the periphery for lower $B = 0.26$ T. In addition, in the low-B regime plasma is more susceptible to magnetohydrodynamic activity resulting in worse transverse confinement and more frequent disruptions. The former is expressed by that the diamagnetic flux D stops growing approximately up to 1 ms before NBI ends. The latter can be observed in figure 4(*f*), where D decreases rapidly after 8 ms.

Nevertheless, confinement under low $B = 0.26$ T has an advantage. As seen in figures 4(*c*) and 2(*b*), diamagnetic flux in the cross-section with local mirror ratio $R = 1.53$, which corresponds to the maximum of the pressure axial profile, undergoes a sharp decrease when AICI arises. Although AICI develops also in the regime with low B, it does not provoke so marked a decrease. In addition, the global sound mode does not

https://doi.org/10.1017/S0022377824000515 Published online by Cambridge University Press

develop under low B: a stair at 6 ms in diamagnetic flux (figure 4f) can be associated with a single half-cycle of global sound mode (GSM). As a consequence, maxima of the fast-ion pressure axial profile remain in the turning points despite AICI.

In addition, a distinction in axial power losses is observed. Axial power losses P_{axial} are measured with a set of pyroelectric bolometers (their design is described in Soldatkina *et al.* (2020)) distributed on the diagnostic plasma absorber (10 in figure 1a). The signals in figures 4(c), 4(f), 6(e) and 6(f) show local power losses integrated over the absorber area; however, there are no data from the on-axis bolometer. The distinction is that AICI does sometimes cause abrupt additional P_{axial} (6.5 ms in figure 4c) with the default magnetic field (5.5 ms in figure 6e), whereas in the case of low B this phenomenon had not been observed at all. Earlier, on-axis energy losses during the AICI were studied by Anikeev *et al.* (2015) in the standard configuration with $B = 0.35$ T. All of this points out that AICI manifests in a milder manner when the magnetic field is low.

3.3. *Configuration with $\delta = 2$*

Initial discharges in magnetic configuration with $\delta = 2$ were exposed to magnetohydrodynamic disruptions as well as at low field with $\delta = 1.5$, but to a greater extent. We were able to stabilise the plasma by reducing the magnetic mirror field strength by 10 % and switching on the reversal magnetic field coil in the western expander region (red dotted arrow in figure 1a). The former action led to a decrease of the radius in the central cross-section of the magnetic surface which touches the limiter from 18.4 to 17.8 cm. This had to decrease the contribution of unfavourable curvature to the criterion against flute instability (Rosenbluth & Longmire 1957). The latter action pushed field lines away from one another in the western expander that contributed to favourable curvature.

Figure 5(a) demonstrates values of $\langle\beta_\perp\rangle$ calculated using formula (3.1) for all three configurations under their default magnetic fields. For the case of $\delta = 2$ this field is $B = 0.24$ T: this value corresponds to the default voltage to which the supplying system of the central solenoid is charged. As can be seen, $\langle\beta_\perp\rangle$ is approximately 0.18 in the $\delta = 2$ configuration, that is, $\approx$2.3 times higher than in the standard configuration. An enhancement of $\langle\beta_\perp\rangle$ in the case of $\delta = 2$ testifies to both the widening of the relatively high $\beta_\perp$ region and, most importantly, a local $\beta_\perp$ increase.

Figure 5(c) shows τ_{decay} values for the same discharges as in figure 5(a), and one can see that the decay time of diamagnetic flux is smaller for $\delta = 2$ than for other configurations even at a moderate fraction of trapped NBI power. This is assumed to be due to transverse transport being more intensive at lower magnetic field, so a comparison at similar values of B is more justified. Green triangles in figure 5(c) are related to confinement in $\delta = 1.5$ and $B = 0.26$ T, which is the closest to the field in $\delta = 2$. In these cases, decay times turn out to be indistinguishable.

In addition, figures 5(b) and 5(d) allow us to compare radial profiles of T_e and n_e. It is visible that near the axis T_e is higher for $\delta = 2$ in comparison to $\delta = 1.5$ with a slightly greater $B = 0.26$ T; however, T_e does not exceed temperatures obtained at higher magnetic fields in other configurations. At the outermost radius temperatures are the same in these cases and higher than in the cases of other configurations and magnetic fields presented above. Whereas, n_e is flat for $\delta = 2$ and density is high enough. Thereby, the quality of energy confinement is better in the configuration with $\delta = 2$ than in that with $\delta = 1.5$ at comparable magnetic fields.

3.4. *Axial distribution of D–D protons*

The fast-ion axial pressure distribution's time dependence can be qualitatively determined using the data on distribution of the fusion reaction products. Thermonuclear D–D proton

https://doi.org/10.1017/S0022377824000515 Published online by Cambridge University Press

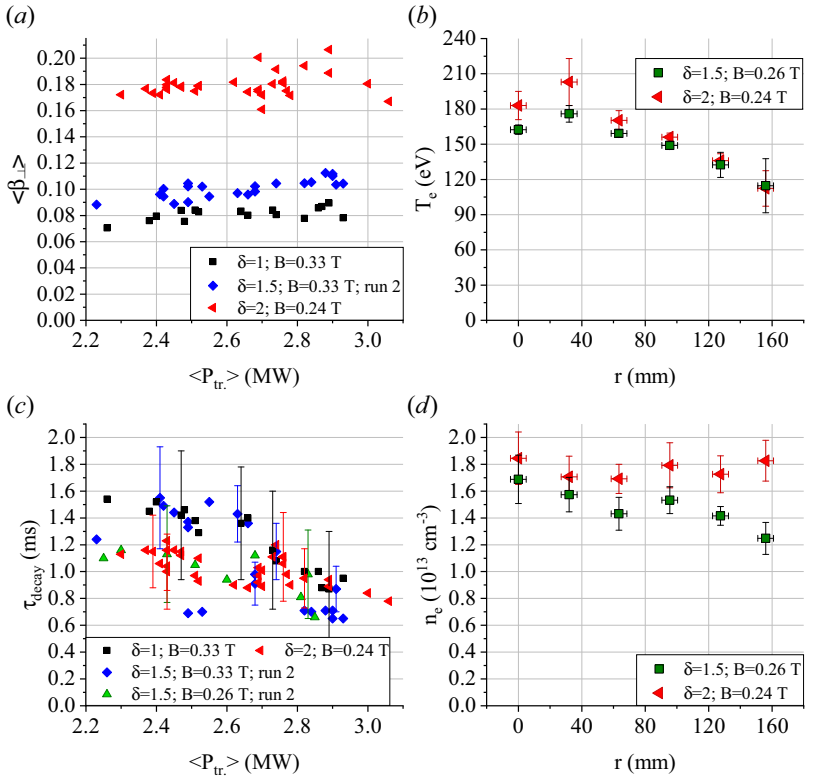

FIGURE 5. Average (*a*) $\beta_\perp$ and (*c*) τ_{decay} for three magnetic configurations. Radial profiles of (*b*) T_e and (*d*) n_e for non-standard configurations with low B.

(3.02 MeV) fluxes were measured by an array of photodiode-based detectors (Pinzhenin & Maximov 2023) distributed along the GDT axis (9 in figure 1*a*). Each detector has a spatial resolution of about several tens of centimetres.

Time dependencies of D–D proton fluxes J_p are presented at the same scale in figure 6(*a–c*) for configurations with δ ranging from 1 to 2. Discharges with similar values of $\langle P_{\text{tr}}\rangle$ were chosen for comparison and each column in figure 6 corresponds to its own discharge. Here $\langle P_{\text{tr}}\rangle$ equals 2.5, 2.6 and 2.7 MW in the same order. Legends in figure 6 are shared in regard to axial coordinates, but the local mirror ratio R relates only to its own graph.

First of all, let us consider dependencies in $\delta = 1$ and $\delta = 1.5$ configurations. Proton fluxes $J_p(t)$ in the central plane are the same. Maxima of $J_p(t)$ (before AICI) are located in the sections with coordinates 175 and 125 cm, respectively. These cross-sections are the closest to both turning points (local mirror ratios of both are equal to 1.9) and the calculated pressure maxima for the related configurations. The AICI arises at ≈6 ms in the configuration with $\delta = 1$ and at ≈5.3 ms in that with $\delta = 1.5$. In both cases near the turning point J_p drops abruptly and becomes equal to the flux in the central cross-section that testifies to the axial pressure profile flattening due to AICI development. In contrast, proton fluxes increase visibly in the sections beyond the turning points. The situation is similar for diamagnetic fluxes. As already mentioned, a sharp rise in P_{axial} can be caused by AICI; however, it is observed occasionally, so AICI more likely provokes mainly the pressure axial redistribution, with no significant losses. For the standard configuration a

https://doi.org/10.1017/S0022377824000515 Published online by Cambridge University Press

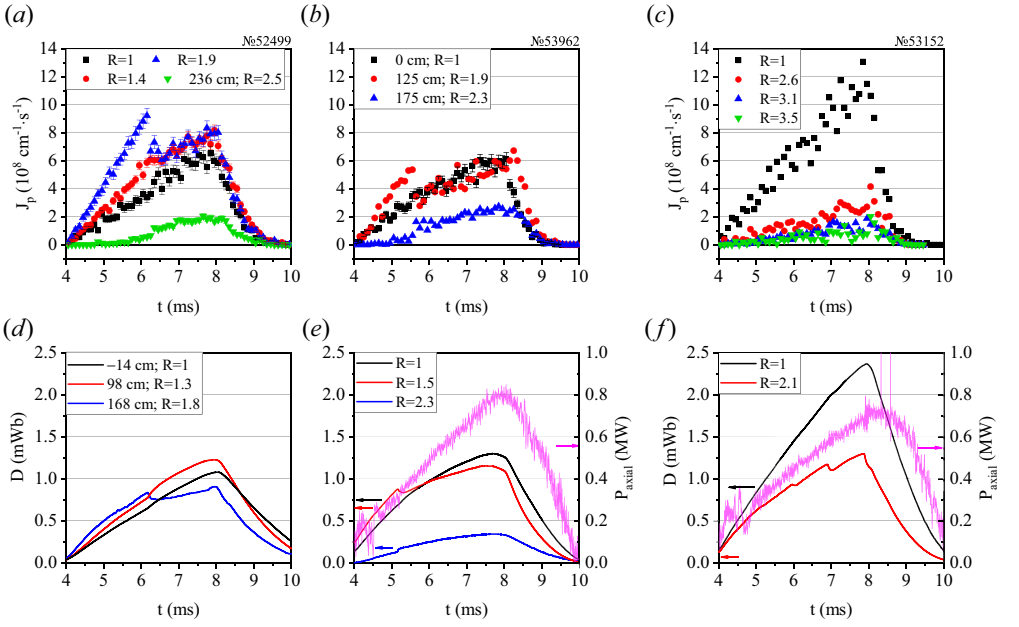

FIGURE 6. Time dependencies of (*a–c*) D–D proton and (*d–f*) diamagnetic fluxes in several plasma cross-sections (defined by local mirror ratio R) for configurations (*a*,*d*) $\delta = 1$, (*b*,*e*) $\delta = 1.5$ and (*c*,*f*) $\delta = 2$. Panels (*e*,*f*) also show axial power losses on the right-hand axes.

low level (about 1 % of P_{tr}) of axial losses caused by AICI was measured in Anikeev *et al.* (2015).

Next, let us draw attention to figures 6(*c*) and 6(*f*). The main feature is J_p in the central plane that is twice as high as proton fluxes in the same plane in both $\delta = 1$ and $\delta = 1.5$ configurations. All cross-sections observed by proton detectors are far from the turning point. Instead, there is a diamagnetic loop at 98 cm that is close to the turning point location ($R = 2.1$). One can see characteristic decreases of diamagnetic flux at ≈6 ms and ≈7 ms when AICI arises, but the flux growth rate does not change after them, unlike in other configurations (figure 6*d*,*e*). Besides, sharp changes of P_{axial} as in figure 4(*c*) have never been observed in the case of $\delta = 2$. These weak arguments evidence that AICI develops in the $\delta = 2$ configuration in a similar way to that under low magnetic field at $\delta = 1.5$ (§ 3.2). If so, fast-ion pressure as well as the D–D proton flux are peaked near the turning points despite the AICI manifesting.

4. Conclusion

This paper is dedicated to the description of general properties of several plasma confinement regimes in the GDT and their comparison to one another. Operation in these regimes is aimed at achieving a maximum possible relative pressure by shrinking the fast ions' movement region.

The following are the most important findings:

(1) Decreasing the distance between the turning points by 1.5 times ($\delta = 1.5$) without changing the central magnetic field leads to an enhancement of $\langle\beta_\perp\rangle$ by 22 % (averaged over the central plasma cross-section).

https://doi.org/10.1017/S0022377824000515 Published online by Cambridge University Press

(2) Reducing the distance by half ($\delta = 2$) but with inevitable change of the central magnetic field from 0.33 to 0.24 T leads to an ≈2.3-fold rise in $\langle\beta_\perp\rangle$ compared with the standard GDT configuration. This is corroborated by a twofold higher D–D proton flux in the central plane for the $\delta = 2$ configuration compared with other configurations. Achieving this confinement regime requires additional measures against the flute instability.

(3) Development of the AICI provokes pressure redistribution along the GDT axis. In the case of default magnetic field ($B = 0.33$ T), the pressure distribution maxima at the turning points are smoothed to a great extent. In the case of low magnetic fields ($B = 0.26$ T) in configuration $\delta = 1.5$, pressure maxima are not found to be smoothed. We need to conduct additional studies to show whether the same is justified for the $\delta = 2$ configuration in which the magnetic field is also low.

The following are the less important findings:

(4) The highest T_e profiles in both $\delta = 1.5$ and $\delta = 2$ configurations have their maxima equal to ≈210 eV, but the former has a temperature of 90 eV at $r = 156$ mm whereas the latter has ≈120 eV at the same radius. In the standard configuration T_e reaches 240 eV near the axis and 90 eV at $r = 156$ mm, where the limiter is projected. Whereas, n_e radial profiles are flat, and densities averaged over the radius are equal to 1.5×10^{13}, 1.8×10^{13} and 1.7×10^{13} cm^{-3} for the $\delta = 1.5$, $\delta = 2$ and standard configurations, respectively. Thereby, confinement of electrons in the $\delta = 2$ configuration is better than in the $\delta = 1.5$ configuration, and is not much worse than in the standard configuration.

(5) The method of increasing the plasma pressure by massive gas puffing and capturing as much NBI power as possible is associated with additional losses of fast ions due to them exchanging charge with excess neutral gas. The optimal fraction of trapped NBI power is equal to ≈65 % when the available method of maintaining target plasma is utilised.

Further studies with direct β measurements in the central plasma cross-section using spectral motional Stark effect diagnostic (Lizunov, Donin & Savkin 2013; Savkin & Lizunov 2017) are being planned.

Acknowledgements

The authors are grateful to members of the GDT team for their collaboration and personally to Dr V.V. Prikhodko for his comments concerning the DOL code.

Editor Cary Forest thanks the referees for their advice in evaluating this article.

Funding

This work was supported by the Ministry of Science and Higher Education of the Russian Federation.

Declaration of interests

The authors report no conflict of interest.

REFERENCES

ANIKEEV, A.V., BAGRYANSKY, P.A., ZAITSEV, K.V., KOROBEINIKOVA, O.A., MURAKHTIN, S.V., SKOVORODIN, D.I. & YUROV, D.V. 2015 Energy spectrum of longitudinal ion losses in the GDT facility under development of Alfvén ion-cyclotron instability. *Plasma Phys. Rep.* **41**, 773–782.

https://doi.org/10.1017/S0022377824000515 Published online by Cambridge University Press

Bagryansky, P.A., Anikeev, A.V., Beklemishev, A.D., Donin, A.S., Ivanov, A.A., Korzhavina, M.S., Kovalenko, Y.V., Kruglyakov, E.P., Lizunov, A.A., Maximov, V.V., *et al.* 2011 Confinement of hot ion plasma with $\beta = 0.6$ in the gas dynamic trap. *Fusion Sci. Technol*. **59** (1T), 31–35.

Bagryansky, P.A., Chen, Z., Kotelnikov, I.A., Yakovlev, D.V., Prikhodko, V.V., Zeng, Q., Bai, Y., Yu, J., Ivanov, A.A. & Wu, Y. 2020 Development strategy for steady-state fusion volumetric neutron source based on the gas-dynamic trap. *Nucl. Fusion* **60** (3), 036005.

Beklemishev, A.D. 2016 Diamagnetic 'bubble' equilibria in linear traps. *Phys. Plasmas* **23** (8).

Beklemishev, A.D., Bagryansky, P.A., Chaschin, M.S. & Soldatkina, E.I. 2010 Vortex confinement of plasmas in symmetric mirror traps. *Fusion Sci. Technol*. **57** (4), 351–360.

Ivanov, A.A. & Prikhodko, V.V. 2017 Gas dynamic trap: experimental results and future prospects. *Phys.-Uspekhi* **60** (5), 509.

Khristo, M.S. & Beklemishev, A.D. 2022 Two-dimensional MHD equilibria of diamagnetic bubble in gas-dynamic trap. *Plasma Phys. Control. Fusion* **64** (9), 095019.

Lizunov, A., Berbasova, T., Khilchenko, A., Kvashnin, A., Puryga, E., Sandomirsky, A. & Zubarev, P. 2023 High resolution Thomson scattering diagnostic for measurements of radial profiles of electron temperature and density in the gas dynamic trap. *Rev. Sci. Instrum*. **94** (3), 033509.

Lizunov, A., Donin, A. & Savkin, V. 2013 Note: spectral motional Stark effect diagnostic for measurement of magnetic fields below 0.3 T. *Rev. Sci. Instrum*. **84** (8).

Pinzhenin, E.I. & Maximov, V.V. 2023 Application of nuclear physics methods for plasma diagnostics in the GDT. *Instrum. Exp. Tech*. (accepted for publication).

Rosenbluth, M.N. & Longmire, C.L. 1957 Stability of plasmas confined by magnetic fields. *Ann. Phys*. **1** (2), 120–140.

Savkin, V.Y. & Lizunov, A.A. 2017 Note: diagnostic deuterium beam with an ultra-small energy spread for plasma spectroscopy. *Rev. Sci. Instrum*. **88** (7).

Simonen, T.C. 2016 Three game changing discoveries: a simpler fusion concept? *J. Fusion Energy* **35**, 63–68.

Skovorodin, D.I., Chernoshtanov, I.S., Amirov, V.K., Astrelin, V.T., Bagryanskii, P.A., Beklemishev, A.D., Burdakov, A.V., Gorbovskii, A.I., Kotel'nikov, I.A., Magommedov, E.M., *et al.* 2023 Gas-dynamic multiple-mirror trap GDMT. *Plasma Phys. Rep*. **49** (9), 1039–1086.

Skovorodin, D.I., Zaytsev, K.V. & Beklemishev, A.D. 2013 Global sound modes in mirror traps with anisotropic pressure. *Phys. Plasmas* **20** (10).

Soldatkina, E.I., Maximov, V.V., Prikhodko, V.V., Savkin, V.Y., Skovorodin, D.I., Yakovlev, D.V. & Bagryansky, P.A. 2020 Measurements of axial energy loss from magnetic mirror trap. *Nucl. Fusion* **60** (8), 086009.

Tsidulko, Y.A. & Chernoshtanov, I.S. 2014 Alfvén ion-cyclotron instability in an axisymmetric trap with oblique injection of fast atoms. *Plasma Phys. Rep*. **40**, 955–964.

Yurov, D.V., Prikhodko, V.V. & Tsidulko, Y.A. 2016 Nonstationary model of an axisymmetric mirror trap with nonequilibrium plasma. *Plasma Phys. Rep*. **42**, 210–225.

Zaytsev, K.V., Anikeev, A.V., Bagryansky, P.A., Donin, A.S., Korobeinikova, O.A., Korzhavina, M.S., Kovalenko, Y.V., Lizunov, A.A., Maximov, V.V., Pinzhenin, E.I., *et al.* 2014 Kinetic instability observations in the gas dynamic trap. *Phys. Scr*. **2014** (T161), 014004.

Zaytsev, K.V., Anikeev, A.V., Bagryansky, P.A., Donin, A.S., Kovalenko, Y.V., Korzhavina, M.S., Lizunov, A.A., Lozhkina, A.N., Maximov, V.V., Pinzhenin, E.I., *et al.* 2013 Magnetic measurements at the GDT facility. *Fusion Sci. Technol*. **63** (1T), 346–348.